J|A|C|S
ARTICLES
Published on Web 04/17/2002

Conformation-Dependent Reaction Thermochemistry: Study of Lactones and Lactone Enolates in the Gas Phase

Joel M. Karty, Gordon A. Janaway, and John I. Brauman*

Contribution from the Department of Chemistry, Stanford University, Stanford, California 94305-5080

Received August 6, 2001

Abstract: Gas-phase acidities ($\Delta H°_{acid}$) of lactones with ring sizes from four to seven have been measured on a Fourier transform ion cyclotron resonance mass spectrometer. Electron affinities (EAs) of the corresponding lactone enolate radicals were measured on a continuous-wave ion cyclotron resonance mass spectrometer, and the bond dissociation energies (BDEs) of the α C−H bonds were derived. In order of increasing ring size, $\Delta H°_{acid} = 368.7 \pm 2.$, 369.4 ± 2.2, 367.3 ± 2.2, and 368.3 ± 2.2 kcal/mol and BDE = 99.4 ± 2.3, 94.8 ± 2.3, 89.2 ± 2.3, and 92.8 ± 2.4 kcal/mol for β-propiolactone, γ-butyrolactone, δ-valerolactone, and ε-caprolactone, respectively. For their corresponding enolate radicals, EA = 44.1 ± 0.3, 38.8 ± 0.3, 35.3 ± 0.3, and 37.9 ± 0.6 kcal/mol. All of these lactones are considerably more acidic than methyl acetate, consistent with a dipole repulsion model. Both BDEs and EAs show a strong dependence on ring size, whereas $\Delta H°_{acid}$ does not. These findings are discussed, taking into account differential electronic effects and differential strain between the reactant and product species in each reaction.

Introduction

Rotational isomers can differ significantly in energy.[1] This does not necessarily mean, however, that the reaction thermochemistry of such isomers will be significantly different. If the energy of the reactant is dependent upon geometry in the same way as the product, we do not expect a large difference in reaction thermochemistry. We investigate here the effects of conformation on the thermochemistry of some simple reactions involving esters and ester enolate species,[2] where we do expect conformation to play a significant role. These reaction thermochemistries, in particular, are the gas-phase Brønsted acidity ($\Delta H°_{acid}$) and the C−H bond dissociation energy (BDE) at the α-carbon of esters, and the adiabatic electron affinity (EA) of ester enolate radicals. This molecular system is experimentally convenient, because the ester functional group can be locked in the *E* conformation in the case of lactones (cyclic esters), whereas in acyclic esters, the closed-shell neutral, the enolate anion, and the enolate radical are all believed to exist primarily in the *Z* conformation (Figure 1).[3,4]

Figure 1. *E* and *Z* rotational isomers of methyl acetate.

Lactones in solution are much stronger acids than esters. In DMSO, the 6-membered ring, δ-valerolactone, is about 5 pK_{HA} units more acidic than ethyl acetate.[5] Meldrum's acid, a cyclic diester, is more than 8 pK_{HA} units more acidic in DMSO than its acyclic analogue, dimethyl malonate.[6] Such phenomena have been explained as a result of an intramolecular dipole−dipole interaction,[7−9] and we revisit this explanation in the discussion. Because these experiments were done in solution, however, solvation effects could complicate the interpretation of the data. We therefore have measured the gas-phase acidities of β-propiolactone (**4H**), γ-butyrolactone (**5H**), δ-valerolactone (**6H**), and ε-caprolactone (**7H**), where the reactions are free from solvent. For each lactone, the acidic proton is at the α-carbon, and the conjugate bases are the enolate anions, $\mathbf{4}^-$, $\mathbf{5}^-$, $\mathbf{6}^-$, and $\mathbf{7}^-$, respectively (Figure 2). We have also employed electron photodetachment spectroscopy to obtain the EAs of the corresponding enolate radicals, **4**•, **5**•, **6**•, and **7**•. BDEs of the neutral lactones were derived, and all experimental results were compared to density functional theory calculations.

We consider the effects of *E* and *Z* conformation on reaction thermochemistry of esters by comparing values from lactone

(1) Lowry, T. H.; Richardson, K. S. *Mechanism and Theory in Organic Chemistry*, 3rd ed.; Harper Collins Publishers: New York, 1987; p 137.
(2) Interpretation of thermochemical measurements of conformational isomers can arise if the isomers are rapidly interchanging (Curtin, D. Y. *Rec. Chem. Prog.* **1954**, *15*, 111; Eliel, E. L. *Stereochemistry of Carbon Compounds*, McGraw-Hill: New York, 1962; pp 151−152 and 237−238). The isomers that we study here, the *E* and *Z* conformations of lactones and lactone enolates, are not rapidly interchanging. Lactone species are locked in the *E* conformation, and the acyclic ester species are all believed to be substantially more stable in the *Z* conformation than in the *E*.
(3) Wiberg, K. B.; Laidig, K. E. *J. Am. Chem. Soc.* **1987**, *109*, 5935.
(4) Our density functional theory calculations suggest that the *Z* conformation of the methyl acetate enolate radical is more stable than the *E* conformation by about 8 kcal/mol.
(5) Arnett, E. M.; Maroldo, S. G.; Schilling, S. L.; Harrelson, J. A. *J. Am. Chem. Soc.* **1984**, *106*, 6759.
(6) Zhang, X. M.; Bordwell, F. G. *J. Org. Chem.* **1994**, *59*, 6456.
(7) Wang, X.; Houk, K. N. *J. Am. Chem. Soc.* **1988**, *110*, 1870.
(8) Wiberg, K. B.; Laidig, K. E. *J. Am. Chem. Soc.* **1988**, *110*, 1872−1874.
(9) In addition see Kyoungrim, B.; Yirong, M.; Gao, J. *J. Am. Chem. Soc.* **2001**, *123*, 3975.

10.1021/ja011897i CCC: $22.00

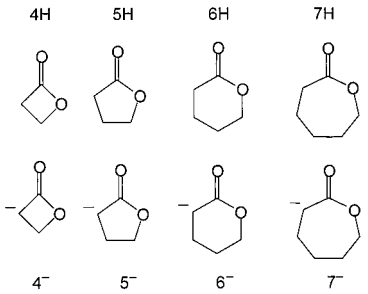

Figure 2. Shorthand notation for lactones and lactone enolates.

and lactone enolates to those of methyl acetate and its enolate species. We also consider the dependence of reaction thermochemistry on ring size, given that the EAs of cyclic ketone enolate radicals have been shown to be very dependent upon ring size.[10] For small rings (<7 carbons), the EA decreases with increasing number of carbons in the ring, while for larger rings, the EA increases. Because of the similar functionality between lactones and cyclic ketones, we look for analogous behavior exhibited by the lactones.

Experimental Section

Materials. Nitrogen trifluoride (NF_3) was purchased from Ozark-Mahoning. Volatile impurities were removed from NF_3 by multiple freeze−pump−thaw cycles. The alcohol and the lactones (all >97% purity) were purchased from Aldrich and used without further purification. Each was pumped directly under vacuum at room temperature in order to degas samples and to remove volatile impurities. In addition, **4H** was transferred under vacuum in order to remove nonvolatile impurities. Each lactone showed only an $M - 1$ mass peak when allowed to react with F^- at short time in the ion cyclotron resonance (ICR) mass spectrometer.

Instrumentation. A Fourier transform ICR (FT-ICR) mass spectrometer[11] with impulse excitation was used to measure the equilibrium acidities. Experiments were performed in a 2-in. cubic cell placed between the poles of an electromagnet, operated at 0.60 T, using IonSpec FTMS electronics and software. Unwanted ions were ejected from the cell by single-frequency excitation at the ion's natural ICR frequency.

Pressures were measured with a Varian 844 vacuum ionization gauge. Low volatility of the alcohol and lactones made it difficult to accurately measure the calibration coefficients for the ionization gauge, and therefore these coefficients were estimated from the molecular polarizabilities[12] determined empirically.[13] The background pressure was 1×10^{-9} Torr, and during experiments, total pressure was about 3×10^{-7} Torr. Reactions were allowed to equilibrate for a minimum of 6 s.

A (cw) ICR[14] was used for all photodetachment experiments, employing continuous excitation and detection. The ICR cell, with a 1 in. square cross section, was placed between the poles of an electromagnet, operated between 0.7 and 1.1 T. Capacitance bridge detection and a frequency lock[15] allowed for measurement of <1% change in steady-state ion population. Background pressure was 5×10^{-9} Torr, and total pressure during experiments was about 2×10^{-7} Torr. Average trapping times of the ions were about 1 s.

The light source for the low-resolution photodetachment experiments was a 1000 W xenon arc lamp (Schoeffel). Wavelengths were selected by a 0.25 m focal length monochromator (Spectral Energy) with a visible grating (350−850 nm). Using 7.7 mm slits, the bandwidth was 25 nm (fwhm). The monochromator was calibrated with a Beck reversion spectroscope, accurate to about 1 nm. Relative power was measured by focusing the exit light from the monochromator into a thermopile (Eppley Laboratory, Inc.) and recording the output voltage.

A tunable cw Ti:sapphire laser (Lexel) was the light source for the high-resolution photodetachment experiments that required wavelengths longer than 695 nm. For experiments at shorter wavelengths, the light source was a Coherent model 590 dye laser with DCM Special laser dye. Both lasers were pumped by a cw Ar ion laser (Coherent) operated in the multiline mode. Wavelengths were selected with a three-plate birefringent filter, giving an overall bandwidth of <40 GHz (about 0.05 nm). The birefringent filter was itself calibrated against the reversion spectroscope, making the wavelength readings accurate to ±1 nm. About 3% of the laser light was split off and directed into the thermopile for relative power measurements.

Acidities. All experiments to determine acidities were performed in the FT-ICR. Fluoride anion, the primary ion, was generated by dissociative electron attachment to nitrogen trifluoride (eq 1). Next, 2,2-dimethyl-3-pentoxide (RO^-) was formed by deprotonating ROH (eq 2), and each lactone was separately allowed to equilibrate with RO^- (eq 3). AH is the neutral ester or lactone, and A^- is the corresponding enolate anion. The equilibrium constant for each reaction was computed by use of eq 4, where P is the pressure of the neutral gas, and I is the ion signal intensity.

$$NF_3 + e^- \rightarrow F^- + NF_2 \quad (1)$$

$$F^- + ROH \rightarrow HF + RO^- \quad (2)$$

$$AH + RO^- \rightleftharpoons ROH + A^- \quad (3)$$

$$K_{eq} = \left(\frac{P_{ROH}}{P_{AH}}\right)\left(\frac{I_{A^-}}{I_{RO^-}}\right) \quad (4)$$

After sufficiently long time (eq 3), the RO^- ion was ejected and equilibrium was reestablished. The steady-state ion intensity ratio after ejection of RO^- was compared to that before ejection to ensure that true equilibria were attained in both cases. Equilibrium constants were converted to relative acidities, $\Delta G^\circ_{acid,rel}$ (eq 5), assuming a cell temperature of 350 K.[11]

$$\Delta G^\circ_{acid,rel} = -RT \ln K_{eq} \quad (5)$$

Absolute acidities, $\Delta G^\circ_{acid,abs}$, were obtained by anchoring the relative acidities to the absolute acidity of the reference alcohol.

The uncertainties in the absolute acidities are taken to be ±2.2 kcal/mol. Significant contributions to this overall uncertainty come from three sources. Estimation of the calibration coefficients for the ionization gauge is accurate to within about 20%.[16] Anchoring our measured values to the acidity of ROH carries with it an uncertainty of ±2.1 kcal/mol (NIST database).[17] Finally, volatile impurities would lead to erroneously high partial pressure readings of the compounds of interest. The contribution from the last source of error is difficult to quantify. However, when the experiments were repeated on different days, a difference of less than 15% was measured in the equilibrium ion intensity ratios. A modest estimate of the error in pressure readings due to volatile impurities would therefore be 20%.

Relative acidities are taken to be significantly more accurate, at ±0.4 kcal/mol. First, the errors introduced from estimating calibration coefficients are slightly reduced, because the linear regression in the relationship between polarizability and ionization gauge sensitivity is

(10) Zimmerman, A. H.; Jackson, R. L.; Janousek, B. K.; Brauman, J. I. *J. Am. Chem. Soc.* **1978**, *100*, 4674.
(11) Han, C. C.; Brauman, J. I. *J. Am. Chem. Soc.* **1989**, *111*, 6491.
(12) Bartmess, J. E.; Georgiadis, R. M. *Vacuum* **1983**, *33*, 149.
(13) Miller, K. J. *J. Am. Chem. Soc.* **1990**, *112*, 8533.
(14) Smyth, K. C.; Brauman, J. I. *J. Chem. Phys.* **1972**, *56*, 1132.
(15) Marks, J.; Drzaic, P. S.; Foster, R. F.; Wetzel, D. M.; Brauman, J. I.; Uppal, J. S.; Staley, R. H. *Rev. Sci. Instrum.* **1987**, *58*, 1460. Modifications to be published.
(16) Estimated from least-squares parameters of the data in ref 12.
(17) Bartmess, J. E. In *NIST Chemistry WebBook, NIST Standard Reference Database 69*; Mallard, W. G., Linstrom, P. J., Eds.; National Institute of Standards and Technology: Gaithersburg, MD, 1998.

Table 1. Experimental and Calculated (B3LYP/6-31+G*) Thermochemistry

species	K_{eq}[b]	$\Delta G°_{acid,exp,rel}$[b]	$\Delta G°_{acid,exp,abs}$[b] (kcal/mol)	$\Delta H°_{acid,exp,rel}$[b] (kcal/mol)	$\Delta H°_{acid,exp,abs}$[b,c] (kcal/mol)	radical EA_{exp}[d] (kcal/mol)	BDE_{exp}[e] (kcal/mol)	$\Delta H°_{acid,calc,abs}$ (kcal/mol)	radical EA_{calc} (kcal/mol)	BDE_{exp}[e] (kcal/mol)	radical and neutral dipoles (D)
ROH[a]		0	362.2 ± 2.2								
4H	114	−2.7 ± 0.4	359.5 ± 2.2	−0.7 ± 0.4	368.7 ± 2.2	44.1 ± 0.3	99.4 ± 2.3	368.7	43.0	98.3	4.7, 4.5
5H	30	−1.8 ± 0.4	360.4 ± 2.2	0	369.4 ± 2.2	38.8 ± 0.3	94.8 ± 2.3	368.8	36.7	92.1	5.5, 5.0
6H	477	−3.8 ± 0.4	358.4 ± 2.2	−2.1 ± 0.4	367.3 ± 2.2	35.2 ± 0.3	89.2 ± 2.3	368.2	34.8	89.6	5.5, 5.0
7H	135	−3.0 ± 0.4	359.2 ± 2.2	−1.1 ± 0.4	368.3 ± 2.2	37.7 ± 0.7	92.8 ± 2.4	368.6	36.9	92.1	5.4, 5.0
$CH_3CO_2CH_3$					371.8 ± 2.1[f]	38.7 ± 0.7	97.1 ± 2.5	371.3[g]	36.5[g]	95.9[g]	1.9, 1.9[g]

[a] 2,2-Dimethyl-3-pentanol. [b] Equilibrium measurement, this work. [c] Anchored to acidity of 2,2-dimethyl-3-pentanol, ref 17. [d] Electron photodetachment, this work. [e] Equation 9. [f] Reference 17. [g] *Z* conformation.

improved when the species contain the same functional groups.[12] Additionally, there is no need to anchor the values. The greatest source of error, then, is that arising from measurements of the partial pressures.

Photodetachment Data. All photodetachment experiments were conducted in the cw ICR mass spectrometer. Fluoride ion was the primary ion (eq 1), and the enolate anions, A^-, were formed via direct deprotonation of the lactones by F^- (eq 6).

The fractional decrease of the ion signal intensity with light was measured for each wavelength, λ. Fractional decreases were caused by the photodestruction of the enolate anion (eq 7); $\mathbf{A}^{\cdot}$ is the resulting enolate radical. Relative cross sections, $\sigma_{rel}(\lambda)$ were then calculated from eq 8, where P is the relative power of the incident light and FD is the fractional decrease.

$$AH + F^- \rightarrow A^- + HF \quad (6)$$

$$h\nu + A^- \rightarrow A^{\cdot} + e^- \quad (7)$$

$$\sigma_{rel}(\lambda) = FD/[\lambda P(1 - FD)] \quad (8)$$

Radical EAs were determined from the photodetachment spectra of the corresponding anions, in which $\sigma_{rel}(\lambda)$ is plotted as a function of λ. Data were taken every 10 nm for the low-resolution spectra. For the high-resolution spectra, data were acquired about every 1 nm to comprise regions of 10−15 nm. Adjacent regions had 3 nm of overlap and were spliced together to form the complete spectrum. For both the low- and high-resolution experiments, each data point represents the average of at least five scans. Maximum fractional decrease was about 15%, and the minimum detectable fractional decrease was about 0.5%.

The energy of light effecting the transition from the ground-state anion to the ground-state radical in eq 7 is the EA of the radical species. The EA of each lactone enolate radical was determined through interpreting its photodetachment spectrum; see Results.

Calculations. Optimized geometries, energies, and dipole moments of all species were obtained from density functional theory calculations (Gaussian 94) at the B3LYP/6-31+G* level of theory. Vibrational frequency calculations were performed on the optimized geometries to obtain entropies, zero-point energies, and thermal corrections.

The calculated $\Delta H°_{acid}$ for each acid was obtained by subtracting the thermally corrected enthalpy of the acid from the sum of the thermally corrected enthalpies of the anion and proton. The calculated EA for each radical species was obtained by subtracting the thermally corrected energy of the anion from that of the radical. The calculated BDEs were derived from a thermochemical cycle, by use of the values for $\Delta H°_{acid}$ and EA (eq 9), where IP(H•) is the ionization potential of the hydrogen atom.

$$BDE = EA(radical) + \Delta H°_{acid} - IP(H^{\cdot}) \quad (9)$$

Results

Acidities. Attempts were made to measure direct proton-transfer equilibria between pairs of lactones with F^- as the base from which to prepare the enolate ions. After initial equilibration, however, subsequent ejection of one enolate ion did not lead to reequilibration to the same steady-state ion intensity ratio. We believe this to be the case for two reasons: (1) Direct proton transfer is too slow for the time scale of these experiments[18] and (2) reaction of F^- with each lactone led to the formation of both the enolate and a highly stable carboxylate ion (eq 10).[19] The carboxylate ion and the enolate ion have identical masses and therefore contribute to the same mass peak in the spectra. The ion concentration ratios therefore do not represent an equilibrium ratio, thus precluding this method of enolate ion preparation for use in equilibrium studies.

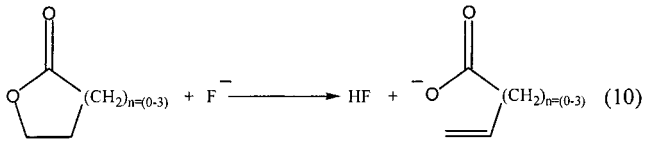

(10)

Preparing the enolate ions with RO^- as the base (eqs 2 and 3) did result in the same steady-state ion concentration ratios both before and after ejection of RO^-. This is an indication that we were observing true equilibria for these acid/base reactions.[20] We therefore calculated the equilibrium constants and $\Delta G°_{acid}$ using the data from these experiments. The equilibrium acidity results are listed in Table 1.

Values for $\Delta H°_{acid}$ were calculated from $\Delta G°_{acid}$ and $\Delta S°_{acid}$. For each lactone, $\Delta S°_{acid}$ was calculated by use of density functional theory; the cell temperature was taken to be 350 K.[11] Relative and absolute $\Delta H°_{acid}$ values are shown in Table 1. Values for methyl acetate, $CH_3CO_2CH_3$,[17] are included as a point of reference.

Photodetachment Data. The low-resolution spectrum for the enolate anion of methyl acetate, $^-CH_2CO_2CH_3$, is shown in Figure 3. Both high- and low-resolution spectra for $\mathbf{5}^-$, $\mathbf{6}^-$, $\mathbf{4}^-$, and $\mathbf{7}^-$ are shown in Figures 4−7, respectively. Interpretation of these photodetachment spectra makes use of features corresponding to energies at which there is an opening of a new channel for electron detachment. Such features include the first nonzero cross section, sharp increases in slope, and narrow resonances near threshold (high-resolution spectra only) that represent transitions to vibrational levels of dipole-bound states (DBS), discussed below. If the adiabatic EA is assigned at one

(18) These observations are consistent with those from Farneth, W. E.; Brauman, J. I. *J. Am. Chem. Soc.* **1976**, *98*, 7891.

(19) We believe that the carboxylate ion is formed because hydrogen sulfide (H_2S), whose acidity lies between that of the lactone and the corresponding carboxylic acid, does not react quantitatively with the ($F^- + nH$) product to give SH^-.

(20) Differential rates of ion loss of those ions involved in the proton transfer equilibrium can significantly perturb the equilibrium measurement if the rate of ion loss is fast compared with the rate of proton transfer. In our experiments, however, the rate of proton transfer, in both the forward and reverse direction, has been observed to be sufficiently fast for each reaction that any such perturbation will be well within the uncertainties that arise from other sources.

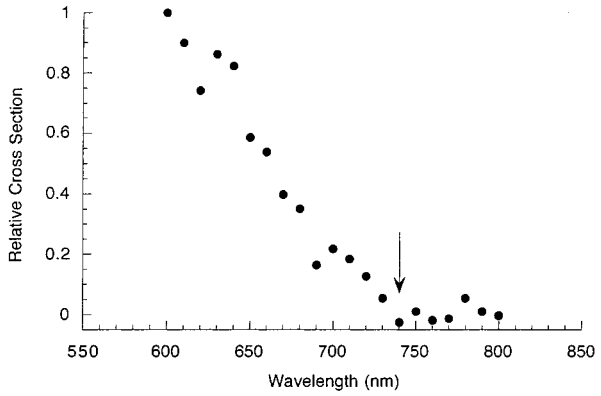

Figure 3. Low-resolution photodetachment spectrum of the enolate anion of methyl acetate. The arrow denotes the assigned onset for the adiabatic electron affinity.

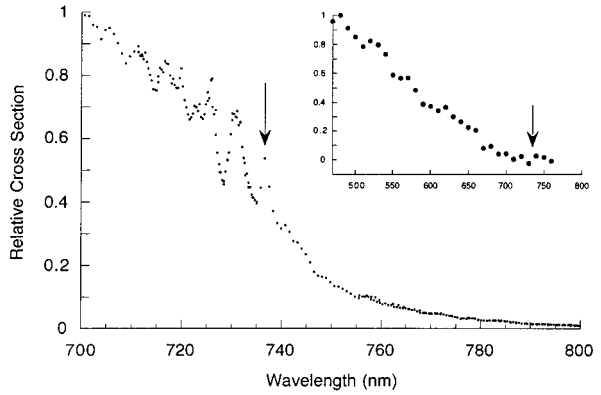

Figure 4. High-resolution photodetachment spectrum of γ-butyrolactone enolate ion ($\mathbf{5}^-$). The inset is the low-resolution spectrum. In each spectrum, the arrow represents the assigned onset.

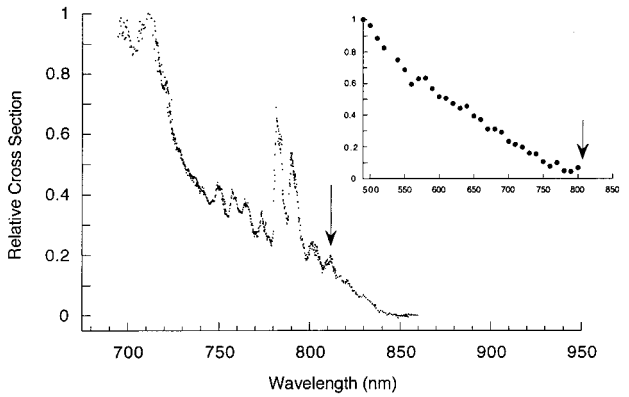

Figure 5. High-resolution photodetachment spectrum of δ-valerolactone enolate ion ($\mathbf{6}^-$). The inset is the low-resolution spectrum. In each spectrum, the arrow represents the assigned onset.

of the latter two features, nonzero cross sections at lower energies are attributed to hot bands, where the electronic transitions occur from vibrationally excited anions.

Dipole-bound states, which can be viewed as the result of an interaction between an electron and a neutral core whose dipole is greater than 1.625 D, were first predicted in 1947 by Fermi and Teller.[21] Since then, there has been much experimental work demonstrating the existence of these electronic states.[22−25] Later experimental work showed that the ground vibrational and rotational state of the dipole-bound state of enolate anions is

(21) Fermi, E.; Teller, E. *Phys. Rev.* **1947**, *72*, 399.

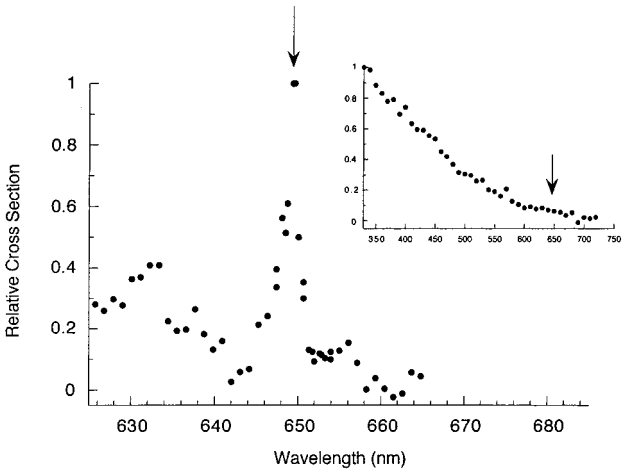

Figure 6. High-resolution photodetachment spectrum of β-propiolactone enolate ion ($\mathbf{4}^-$). The inset is the low-resolution spectrum. In each spectrum, the arrow represents the assigned onset.

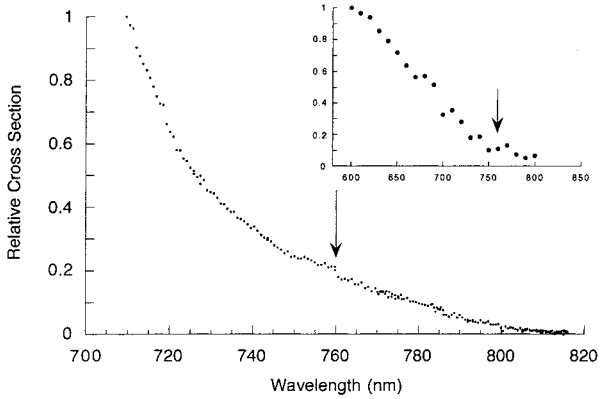

Figure 7. High-resolution photodetachment spectrum of ϵ-caprolactone enolate ion ($\mathbf{7}^-$). The inset is the low-resolution spectrum. In each spectrum, the arrow represents the assigned onset.

typically bound by only tens of wavenumbers.[26−28] This often makes the lowest energy resonance in a photodetachment spectrum a lower bound for the adiabatic EA. Assuming the Franck−Condon overlap between the ground-state anion and the dipole-bound state is sufficiently large, the transition between these two states should be optically accessible and therefore should be very near the adiabatic EA.

Because similar features were not shared among all the high-resolution spectra, each spectrum is interpreted separately below. The EAs and the derived BDEs are listed in Table 1.

Methyl Acetate Enolate ($^-CH_2CO_2CH_3$), Figure 3. Linear extrapolation[14] to zero cross section gives 740 ± 13 nm as the onset. This corresponds to an energy of 38.7 ± 0.7 kcal/mol (1.68 ± 0.03 eV) as the EA.

γ-Butyrolactone Enolate ($\mathbf{5}^-$), Figure 4. In the low-resolution spectrum, linear extrapolation to zero cross section

(22) Rohr, K.; Linder, F. *J. Phys. B* **1976**, *9*, 2521.
(23) Wong, S. F.; Schulz, G. J. *Phys. Rev. Lett.* **1974**, *33*, 134.
(24) Jackson, R. L.; Zimmerman, A. H.; Brauman, J. I. *J. Chem. Phys.* **1979**, *71*, 2088.
(25) Marks, J.; Comita, P. B.; Brauman, J. I. *J. Am. Chem. Soc.* **1985**, *107*, 3718.
(26) Mead, R. D.; Lykke, K. R.; Lineberger, W. C.; Marks, J.; Brauman, J. I. *J. Chem. Phys.* **1984**, *81*, 4883.
(27) Marks, J.; Brauman, J. I.; Mead, R. D.; Lykke, K. R.; Lineberger, W. C. *J. Chem. Phys.* **1988**, *88*, 6785.
(28) Lykke, K. R.; Neumark, D. M.; Andersen, T.; Trapa, V. J.; Lineberger, W. C. *J. Chem. Phys.* **1987**, *87*, 6842.

suggests the EA to occur at 725 ± 13 nm. In the high-resolution spectrum, there is a sharp increase in slope around 745 nm, and there are multiple sharp resonances, spaced around 90 cm^{-1}.[29] The lowest energy resonance is centered at 737 nm, which is taken to represent the adiabatic EA. The corresponding energy is 38.8 ± 0.3 kcal/mol (1.68 ± 0.01 eV).

***δ*-Valerolactone Enolate (6^-), Figure 5.** Linear extrapolation in the low-resolution spectrum gives 800 ± 13 nm as the threshold. In the high-resolution spectrum, as in that for $\mathbf{5}^-$, multiple resonances appear on top of the rising background, here with a spacing of around 150 cm^{-1}.[30] Only three of these resonances are centered within the uncertainty of the assignment from the low-resolution data: those at 790, 802, and 812 nm. We assign the EA to the resonance at 812 nm so that there is internal consistency with the Franck−Condon factors (FCF) associated with each resonance, as described below.

Because there is only a modest change in calculated geometry (B3LYP/6-31+G*) between $\mathbf{6}^-$ and $\mathbf{6}^{\cdot}$, we expect significant symmetry of the Franck−Condon factors on either side of the 0 ← 0 transition. That is, we expect similar Franck−Condon factors for the 1 ← 0 and 0 ← 1 transitions, for the 2 ← 0 and 0 ← 2 transitions, etc. Furthermore, we believe all resonances in the spectrum arise from the same electronic transition. Therefore, the intensity of each resonance should be nearly proportional to the Franck−Condon factors of that transition, scaled by the population of the ions in the initial vibrational level.

If the resonance at 812 nm represents the 0 ← 0 transition, then the resonance at 802 nm is the 1 ← 0 transition, and the resonance at 821 nm is the 0 ← 1 transition. The similarity of the intensities of the 0 ← 0 and 1 ← 0 transitions suggests that their Franck−Condon factors are also similar. The 0 ← 1 transition is significantly less intense because the population of ions in the $v = 1$ vibrational level is smaller, obeying the Boltzmann relationship of populations. The Boltzmann population of the $v = 2$ level of the ion is smaller than that of the $v = 1$ level, but the resonance corresponding to the 0 ← 2 transition appears to have the same intensity as that corresponding to the 0 ← 1 transition. This is because the Franck−Condon factor for the 0 ← 2 transition appears to be significantly greater. We cannot identify a resonance for the 0 ← 3 transition, because its Franck−Condon factor appears not to compensate for the small population of the $v = 3$ level of the ion.

With relative Franck−Condon factor values as a guide, it is difficult to assign the 0 ← 0 transition to any resonance in the spectrum other than that at 812 nm. The EA is therefore taken to be 35.2 ± 0.3 kcal/mol (1.53 ± 0.01 eV).

***β*-Propiolactone Enolate (4^-), Figure 6.** In the low-resolution spectrum, the cross section appears to reach zero near 700 nm. However, there appear to be two increases in slope at lower wavelength, signifying the opening of new channels for electron detachment: one below around 600 nm and the other below around 480 nm. Extrapolation of each of the three linear regions to zero cross section results in potential onsets at 575 ± 13, 650 ± 13, and 725 ± 13 nm.

Given only the low-resolution data, it is difficult to discern which represents the adiabatic electron affinity. We therefore acquired high-resolution data in the regions surrounding the two potential onsets at longer wavelength: one from 625 to 665 nm with the dye laser and the other from 695 to 850 nm with the Ti:sapphire laser.

The high-resolution spectrum shown is that acquired with the dye laser.[31] The cross section appears to reach zero around 660 nm.[32] One prominent resonance appears at 649 nm and another smaller resonance at 633 nm, both of which we believe represent transitions to dipole-bound states. Of the two resonances, only the one centered at 649 nm is within the uncertainty of the potential onset assignment of 650 ± 13 nm from the low-resolution data. The high-resolution assignment corresponds to an energy of 44.1 ± 0.3 kcal/mol (1.91 ± 0.01 eV).

***ε*-Caprolactone Enolate (7^-), Figure 7.** The low-resolution spectrum suggests an onset of 760 ± 13 nm. In contrast to the previous spectra, this high-resolution spectrum lacks resonances near the onset, thereby precluding use of DBS as a method of assigning the EA. The EA is therefore taken from the low-resolution spectrum to be 37.7 ± 0.7 kcal/mol (1.63 ± 0.03 eV).[33]

Calculations. Calculated thermochemical values and dipole moments are summarized in Table 1. Relevant geometric parameters of lactones and lactone enolates are presented in Table 2. Vertical electron affinities and subsequent relaxation energies (see Discussion) are listed in Table 3. Vertical bond dissociation energies and subsequent relaxation energies (see Discussion) are listed in Table 4.

Table 2. Calculated Bond Angles in Lactone Enolates (B3LYP/6-31+G*).

	calculated ∠O–C–C (Θ), deg	
enolate	radical	anion
4	139.5	144.5
5	129.4	135.9
6	123.1	130.2
7	122.6	131.8
$CH_3CO_2CH_3$	122.0	129.9

Discussion

In this study we investigate the effects of molecular geometry on the thermodynamics of simple reactions involving ester and ester enolate species. We have measured the gas-phase acidities

(29) This regular spacing of the resonances appears to define a vibrational progression. AM1 calculations show two ring-bending modes in the radical neutral, at 168 and 176 cm^{-1}.

(30) AM1 calculations show two ring-bending modes in the vicinity of 150 cm^{-1}, at 101 and 134 cm^{-1}.

(31) In the longer wavelength high-resolution spectrum (not shown), there is a small but nonzero cross section at wavelengths as high as 850 nm, and there is an increase in slope below 750 nm. This slope increase must represent the opening of a new channel for electron detachment. Furthermore, linear extrapolation of the shallower slope in the low-resolution spectrum appears to reach zero cross section in this vicinity. Although an argument can be made to assign the EA in this region, we do not assign it there, for two reasons: (1) There are no sharp resonances above 695 nm that correspond to transitions to dipole bound states, and (2) an assignment of the EA in the region above 695 nm would lead to significant disagreement with our density functional theory calculations.

(32) Although the region of the photodetachment spectrum acquired with the dye laser shows negligible cross section above 660 nm, a nonzero cross section is measured with the Ti:sapphire laser at significantly longer wavelengths. Largely this is because of the roughly 5-fold higher power output of the Ti:sapphire laser. At small cross sections, this translates into about a 25-fold increase in signal-to-noise in the Ti:sapphire region. With the dye laser as the light source, the nonzero cross sections become buried in the noise at wavelengths longer than about 660 nm.

(33) The high-resolution spectrum contains three linear regions, one below 730 nm, one between 730 and 750 nm, and another above 750 nm. Linear extrapolation of each linear region to zero cross section leads to 740, 770, and about 800 nm as the possible onsets. Assignment of the EA at 800 or 740 nm would be outside the uncertainty in the assignment from the low resolution spectrum. Assignment at 770 nm, on the other hand, would fall within the limits of uncertainty of the low-resolution assignment.

Table 3. Calculated Vertical Electron Affinities and Relaxation Energies of Lactone Enolate Radicals (B3LYP/6-31+G*)

	relative calculated energies (kcal/mol)	
lactone enolate anion	EA_{vert}	$\Delta E_{relax,EA}$
4$^-$	48.4	5.5
5$^-$	43.4	6.7
6$^-$	41.0	6.2
7$^-$	44.0	7.1

Table 4. Relative Calculated Vertical Bond Dissociation Energies and Relaxation Energies of Lactones (B3LYP/6-31+G*)

	relative calculated energies (kcal/mol)	
lactone	BDE_{vert}	$\Delta E_{relax,BDE}$
4H	106.1	9.3
5H	105.5	10.7
6H	101.2	12.0
7H	102.0	9.2

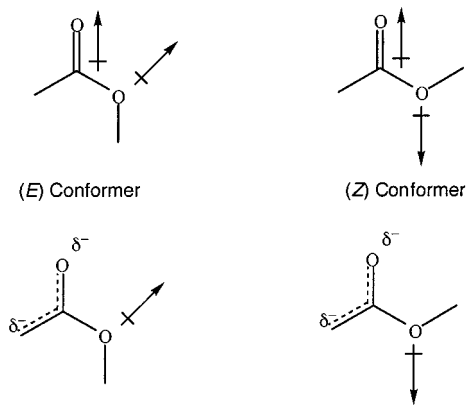

Figure 8. Methyl acetate (top) and its enolate anion (bottom). Dipole repulsion in the neutral leads to destabilization in the *E* conformation relative to the *Z* conformation. This effect is diminished in the enolate anion.

of lactones with ring sizes from 4 to 7. We have also measured the EAs of the corresponding enolate radicals, and we derived the lactone α C−H bond dissociation energies. Comparisons are made between these values, representative of the ester *E* conformation, and those involving methyl acetate species, which are representative of the ester *Z* conformation. Results from experiments are supplemented by density functional theory calculations.

Few species have been studied in which reaction thermochemistry is dependent upon conformation. Römer and Brauman[34] measured the EA of the enolate anion of propionaldehyde in the *Z* conformation to be about 2 kcal/mol higher than that in the *E* conformation. Gandour[35] and Rebek and co-workers[36] showed that, in solution, carboxylic acids are more acidic by 1−3.9 kcal/mol when the proton is in the syn conformation as opposed to the anti. Both of these studies, however, are of processes that involve two conformations of reactants that lead to a single product conformation. The present study, on the other hand, involves reactions in which the reactant and the product have the same conformation.

Acidities. In their studies of the enhanced solution acidity of Meldrum's acid over dimethyl malonate, both Wang and Houk[7] and Wiberg and Laidig[8] observed that (*E*)-methyl acetate is calculated to be about 5 kcal/mol more acidic than (*Z*)-methyl acetate. These results have been explained by a dipole repulsion model, in which conformational stability is largely determined by the electrostatic interaction of group dipoles and charges in the lactone and lactone enolate species.[7,8]

The dipole repulsion model takes into account the primary group dipole contributions to the net molecular dipole in the neutral lactone: that from the carbonyl group and that originating from the lone pairs of electrons on the ether oxygen. In (*E*)-methyl acetate, these group dipoles are nearly parallel (Figure 8), giving rise to an overall repulsive interaction. In (*Z*)-methyl acetate, the dipoles are essentially antiparallel, thereby providing an overall stabilizing effect. In the enolate anion, on the other hand, there is significant charge density on both the carbonyl oxygen and the α-carbon atoms. Therefore, the group dipole from the ether oxygen encounters electrostatic repulsion in both the *E* and *Z* conformations. As a result, the energy difference between the two conformations in the enolate anion is less than that in the neutral acid, which gives rise to the greater acidity of (*E*)-methyl acetate over (*Z*)-methyl acetate.

Density functional theory calculations (B3LYP/6-31+G*) are consistent with the predictions of the dipole repulsion model.[37] (*E*)-Methyl acetate is calculated to be 7.7 kcal/mol higher in energy than (*Z*)-methyl acetate. The enolate anion of (*E*)-methyl acetate, however, is calculated to be only 2.5 kcal/mol higher in energy than the enolate anion of (*Z*)-methyl acetate. Therefore, (*E*)-methyl acetate is calculated to be 5.2 kcal/mol more acidic than (*Z*)-methyl acetate.

The 4−7-member ring lactones and lactone enolates are all *E* esters. Therefore, the dipole repulsion model would predict that the acidities of lactones should all be enhanced relative to that of methyl acetate. In particular, the acidity of **6H** should be nearly the same as that of (*E*)-methyl acetate because the differential strain about the ester group upon deprotonation appears to be similar for the two species. That is, the calculated geometry surrounding the ester group in each acid is nearly identical, and the same is true for the ester enolate group in each anion. Indeed, the acidities of the lactones we have studied are all stronger than the acidity of methyl acetate by 2.4−4.5 kcal/mol (Table 1). Furthermore, **6H** is 4.5 kcal/mol more acidic than (*Z*)-methyl acetate, which is close to the 5.2 kcal/mol calculated acidity enhancement of (*E*)-methyl acetate over (*Z*)-methyl acetate. The dipole repulsion model is therefore consistent with the acidity observations of lactones versus methyl acetate.

All four lactones are quite similar in acidity (Table 1, Figure 9). The range is only 2.1 kcal/mol, with **6H** being the most acidic. A simple picture presents these small ring lactones as only *E* esters, and would argue that their acidities should be nearly the same. However, given the large range (about 9 kcal/mol) in electron affinities of the lactone enolate radicals (Table 1), the picture cannot be this simple. Instead, it appears that there are a number of opposing effects that compensate one another (eq 9) so as to result in an acidity that is insensitive to ring size. Possible effects that govern the acidities of the different

(34) Römer, B. C.; Brauman, J. I. *J. Am. Chem. Soc.* **1997**, *119*, 2054.
(35) Gandour, R. D. *Bioorg. Chem.* **1981**, *10*, 169.
(36) Tadayoni, B. M.; Huff, J.; Rebek, J. *J. Am. Chem. Soc.* **1991**, *113*, 2247.

(37) Calculations on the neutral and the anion were originally performed by Wang, X.; Houk, K. N. *J. Am. Chem. Soc.* **1988**, *110*, 1870 (6-31+G*//3-21G) and Wiberg, K. B.; Laidig, K. E. *J. Am. Chem. Soc.* **1987**, *109*, 5935 (MP3/6-31G**//6-31G*). Our calculations, optimized at B3LYP/6-31+G*, are in agreement with these.

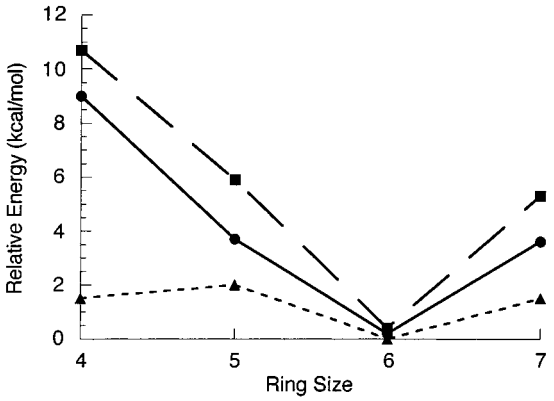

Figure 9. Acidity (▲), EA (●), and BDE (■) as functions of ring size. The values for EA and BDE show a strong dependence on ring size, while the acidity does not.

lactones include (1) geometry dependence of the electrostatic interactions of the dipole repulsion model, (2) polarizability of the anions, (3) differential skeletal strain within the rings, and (4) strain of the π system in the enolate anions.[10] We examine each of these effects on lactone acidity.

We believe that the differences in the electrostatic interactions among the lactones have a negligible effect on the acidities. The calculated dipole moments of the neutral acids are all similar (Table 1). The range is only about 10%, suggesting that the electrostatic repulsive interactions are similar in each lactone. If, on the other hand, these differences in net dipole moment reflected large differences in electrostatic repulsion, the dipole repulsion model would predict the order of electron affinities within the lactone enolate radicals to be different than what is observed. A more detailed explanation is presented later in the treatment of electron affinities.

Anion polarizability should enhance the acidity of the larger rings. The larger rings are greater in mass and therefore are more polarizable. The additional polarizability provides additional internal solvation of the negative charge in anions and therefore effectively stabilizes the conjugate bases of the lactones.[38]

The differential strain in the framework of the rings upon deprotonation should lead to a greater acidity in the larger ring lactones. Primarily this is due to the strain introduced in the rehybridization of the α-carbon from sp^3 to sp^2 in the enolate anion. In each ring, this rehybridization causes an additional 10.5° of angular strain within the ring,[39] and the resulting strain energy is worse for smaller rings.[40] Additionally, larger rings are not constrained to be planar and can better compensate for the introduced strain through out-of-plane relaxation. Smaller ring anions are therefore effectively destabilized, resulting in weaker conjugate acids.

(38) Brauman, J. I.; Blair, L. K. *J. Am. Chem. Soc.* **1968**, *90*, 6561.
(39) The assumption is that rehybridization occurs without a change in geometry of the ring. We define the strain angle to be the difference between the sum of the ideal bond angles and the sum of the internal angles of that ring. The ideal bond angle in an sp^3 center is about 109.5°, and that in an sp^2 center is 120°. If, in a planar ring, an sp^3 center is replaced with an sp^2 center, then the sum of the ideal bond angles is increased by 10.5°, whereas the sum of the internal angles is unchanged. The total angular strain of that ring is therefore increased by 10.5°.
(40) In the harmonic oscillator limit, energy is quadratic in the bond angle, Θ. Consequently, an increment of Θ causes a larger increment in energy when Θ is farther from equilibrium. In the smaller rings, Θ is farther from ideal, and therefore 10.5° additional angular strain represents more added strain energy than in larger rings.

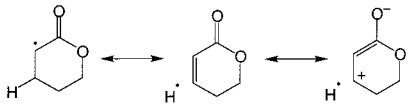

Figure 10. Resonance structures of the enolate radical of δ-valerolactone. Hyperconjugation with the β-carbon and extended resonance stabilize the radical.

Differences in π system strain within the lactone enolate anions tend toward stronger acidity in smaller rings. An antibonding interaction between the O and C ends of the enolate anion moiety is decreased in the smaller rings, because the OCC angles are constrained to be larger (see discussion on electron affinities).[10] The anion is therefore effectively stabilized with smaller ring size, and the conjugate acid is stronger.

We believe that the 4−7-member ring lactones are similar in acidity due to competing effects with ring size. These effects are more clearly seen with the following individual treatment of electron affinities and bond dissociation energies with ring size.

Electron Affinities. Density functional theory calculations (B3LYP/6-31+G*) suggest that the electron affinity of the enolate radical of (*E*)-methyl acetate is 5.3 kcal/mol greater than that of (*Z*)-methyl acetate. The dipole repulsion model accounts for this result. The major contributions to the net molecular dipole in the enolate radical of methyl acetate are similar to those in the neutral acid. Therefore, the dependence of energy on conformation in the enolate radical of methyl acetate should be similar to that in methyl acetate. Density functional theory calculations are consistent with these predictions, suggesting that the enolate radical of methyl acetate is 7.8 kcal/mol higher in energy in the *E* conformation than in the *Z* conformation. The diminished sensitivity to conformation in the enolate anion of methyl acetate (2.5 kcal/mol) gives rise to the 5.3 kcal/mol higher calculated EA in the *E* conformation.

The EA of the enolate radical of methyl acetate in the *Z* conformation is measured to be about 3 kcal/mol higher than the EA of **6·**. If the EA of the enolate radical of methyl acetate in the *E* conformation is higher by an additional 5 kcal/mol, then it would be about 8 kcal/mol higher than that of **6·**. This is in agreement with density functional theory calculations, which suggest that the EA of the methyl acetate enolate radical in the *E* conformation is 7.0 kcal/mol higher than that of **6·**. However, the dipole repulsion model alone predicts that the EA of **6·** should be nearly the same as that of the enolate radical of methyl acetate in the *E* conformation; the geometries of the ester enolate moieties in both radicals are nearly identical, and the same is true for both anions.

This difference in the EAs of the *E* conformation of the methyl acetate enolate radical and **6·** appears to arise from a stabilizing effect by the β-carbon in **6·** that is not present in the enolate radical of methyl acetate. The β-carbon allows for a hyperconjugative interaction with the orbital holding the odd electron.[41] Extended conjugation with the π system of the carbonyl group has been suggested to provide more stabilization than hyperconjugation alone [42−44] (Figure 10).

(41) Bordwell, F. G.; Harrelson, J. A., Jr. *Can. J. Chem.* **1990**, *68*, 1714.
(42) Balaban, A. T. *Rev. Roum. Chim.* **1971**, *16*, 725.
(43) Baldock, R. W.; Hudson, P.; Katritzky, A. R.; Sati, F. *J. Chem. Soc., Perkin Trans. 1* **1974**, *12*, 1422.
(44) Viehe, H. G.; Janousek, Z.; Merényi, R.; Stella, L. *Acc. Chem. Res.* **1985**, *18*, 148.

Figure 11. Enolate radical of propionic acid in the (*E*,*E*′) conformation.

This β-carbon effect is reflected in the α C−H bond dissociation energies of carbonyl compounds, and in the EAs of their enolate radicals. Bordwell and Harrelson[41] have shown that in DMSO the bond dissociation energy of 3-pentanone is about 6 kcal/mol lower than that of acetone. In the gas phase, Römer and Brauman[34] have measured the EA of the enolate radical of (*E*)-propionaldehyde to be about 5 kcal/mol less than that of acetaldehyde.[26] The β-carbon effect therefore appears to be worth about 5−6 kcal/mol stabilization of the enolate radical.

If the β-carbon effect is taken into account with the dipole repulsion model, we would predict the EA of the enolate radical of methyl acetate in the *Z* conformation to be about the same as the EA of **6**·. This is because the β-carbon effect and the dipole repulsion in **6**· have opposite effects on the EA that are roughly of the same magnitude. That is, dipole repulsion is expected to increase the EA of **6**· relative to that of the (*Z*)-methyl acetate enolate radical by about 5 kcal/mol, whereas the β-carbon effect is expected to decrease the relative EA of **6**· by about 5−6 kcal/mol. Additionally, we would predict that an appropriate species to accurately model the EA of **6**· would be the enolate of (*E*,*E*′)-propionic acid (Figure 11). This species is an *E* ester that contains a β-carbon.

Our results are in good agreement with these predictions. The experimental EA of the methyl acetate enolate radical is only about 3 kcal/mol higher than that of **6**·. Furthermore, the difference in the calculated EA of **6**· and the enolate radical of (*E*,*E*′)-propionic acid is only 0.5 kcal/mol. This suggests that in **6**· the β-carbon effect and the electrostatic repulsion of the ester *E* conformation are in opposition and are roughly the same magnitude.

As opposed to the lactone acidities, the EAs of the lactone enolate radicals vary widely with ring size. These values span about 9 kcal/mol (Table 1, Figure 9); the maximum EA is that of **4**·, the minimum EA is that of **6**·, and the EA of **5**· is about the same as that of **7**·. Calculations are in excellent agreement with these results (Table 1).

Similar to our observations with neutral lactones, the calculated dipole moments of the lactone enolate radicals do not vary greatly with ring size (Table 1). Consequently, the dependence on geometry of the electrostatic interactions within the radicals is believed to be small. Were the electrostatic interactions to have a strong dependence on geometry, we would expect the dipole repulsion to be weakest in **4**·, because it has the smallest net dipole moment. Consequently, we would expect **4**· to have the lowest EA. Instead, we observe that **4**· has the highest EA by several kilocalories per mole. We therefore believe that the dependence of the electrostatic interactions on geometry does not contribute significantly to the function of EA with ring size.

Polarizability would tend to increase the EA of the larger ring lactones. The larger rings have more mass, and therefore have greater polarizability, thereby providing better stabilization of the enolate anion. The results indeed show that the EA increases from **6**· to **7**·. However, EA decreases from **4**· to **5**· and again from **5**· to **6**·, suggesting that other effects dictate the order of EAs for these compounds.

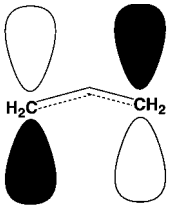

Figure 12. Representation of the allyl HOMO, showing an antibonding interaction between the ends. The enolate analogue has a similar antibonding interaction between its O and C ends.

We must also consider skeletal strain within the rings of lactone enolates as a potential contribution to the function of EA with ring size. We observe that, for each lactone enolate, the calculated geometry of the ring in the radical is very similar to that in the anion.[45] This is different from deprotonation because, unlike deprotonation, electron detachment from an enolate anion does not result in rehybridization at the α-carbon. In both the enolate radical and anion, the α-carbon is sp^2-hybridized. Therefore, little strain is introduced into the ring upon electron detachment. As a consequence, out-of-plane relaxation of the ring not only should be small but also should be very similar for each lactone enolate. Skeletal strain within the rings is therefore expected to contribute little to the function of EA with ring size.

To investigate quantitatively the importance of skeletal strain introduced upon electron detachment, we calculated the vertical EA (EA_{vert}) and the subsequent relaxation energy ($\Delta E_{relax,EA}$) for each lactone enolate (eq 11):

$$\mathrm{EA} = EA_{vert} - \Delta E_{relax,EA} \qquad (11)$$

EA_{vert} is the energy required to remove the electron from the enolate anion, leaving the geometry of the species unchanged. $\Delta E_{relax,EA}$ is the energy released when the vertical product relaxes to the optimized radical geometry. We observe that EA_{vert} tracks the EA, and $\Delta E_{relax,EA}$ is nearly the same for each lactone enolate (Table 3). These observations are consistent with the assertion that skeletal strain in the ring is not important in the function of EA with ring size. This function must therefore be dependent upon another effect.

The π system strain in the enolate anions appears to be an important effect in the function of EA with ring size. As mentioned in the earlier discussion on acidities, there is an antibonding interaction between the O and C ends of the enolate anion. This antibonding interaction is evident in the Hückel representation of the allyl HOMO (Figure 12), which is similar to the enolate HOMO. The greater occupancy of the HOMO in the anion than in the radical increases the antibonding character between the ends of the system, resulting in a more open angle. This effect can be seen in the calculated enolate geometries, where, for each species, the OCC enolate angle is significantly greater in the anion than in the radical (Table 2).

It appears that ring size dictates the calculated lactone enolate OCC angle (Table 2), which, in turn, dictates the π system strain in the enolate anion. In an attempt to quantitatively model the

(45) The interior angles of the 4-, 5-, and 6-membered ring radicals are all within 1° of those of the anions. For the 7-membered ring, there is a difference of about 4° at the carbonyl carbon between the radical and the anion.

effect of ring size on π system strain, we calculated the EA of acyclic enolate species, constraining the angle that corresponds to the interior angle of the carbonyl carbon. Of these acyclic enolate species, the enolate of acetaldehyde is the only one that does not exhibit significant steric strain at the geometry of γ-butyrolactone enolate. Using the enolate of acetaldehyde as a model, we were able to reproduce qualitatively the observed function of EA with ring size. However, we were able to reproduce only about half of the observed magnitude.

In summary, there appear to be two competing effects that determine the function of EA with ring size: π system strain and polarizability of the enolate anions. The minimum in EAs at a ring size of 6 suggests that for smaller rings π system strain dominates, whereas for larger rings polarizability dominates. Modeling π system strain with acetaldehyde enolate appears to account for half of the range of lactone EAs, suggesting that there are other, complicated strain effects that we cannot deconvolute.

Bond Dissociation Energies. Density functional theory calculations suggest that the α C−H bond dissociation energies of methyl acetate in both the *E* and *Z* conformations are nearly identical. Although the energies of methyl acetate and its enolate radical are both highly dependent on conformation, they are both dependent on conformation in the same way. (*E*)-Methyl acetate is calculated to be about 7.7 kcal/mol higher in energy than (*Z*)-methyl acetate, and the energy of the enolate radical of methyl acetate is calculated to be about 7.8 kcal/mol higher in the *E* conformation than in the *Z* conformation. The dipole repulsion model is therefore consistent with these observations.

The experimental bond dissociation energy of methyl acetate (representative of the *Z* conformation) is about 6 kcal/mol higher than that of **6H**. The dipole repulsion model alone suggests that the bond dissociation energies of these esters should be the same. The β-carbon effect, however, stabilizes the radical by about 5 kcal/mol and therefore brings the dipole repulsion model into agreement with our experimental results.

Lactone bond dissociation energies are highly dependent on ring size, spanning almost 10 kcal/mol. Similar to the function of EAs with ring size, the minimum is at a ring size of 6, the maximum is at a ring size of 4, and the 5- and 7-member rings have about the same bond dissociation energy (Table 1, Figure 9). We explain these results through an analysis similar to those employed in the treatments of acidity and EA with ring size.

The dependence of electrostatic repulsion on geometry is negligible in lactones and in their enolate radicals, for reasons outlined in the discussions on acidity and electron affinity. If, however, these dependencies were significant, we would expect the dependence to be the same in both species, due to similar group dipole contributions in each. The effect on bond dissociation energy would then necessarily be quite small.

Both polarizability and π system strain are of little concern in the function of bond dissociation with ring size. Polarizability will have little effect on the stability of either the acid or the enolate radical because neither species is charged. π system strain is much less important in the enolate radical than in the anion; there is less occupancy of the enolate HOMO and therefore less repulsion between the O and C ends. The interaction is altogether absent in the closed-shell neutral lactones.

To model the importance of skeletal strain of the ring on the function of bond dissociation energy with ring size, we have calculated the vertical bond dissociation energy (BDE_{vert}) and the subsequent relaxation energy ($\Delta E_{relax,BDE}$) for each lactone (eq 12). BDE_{vert} is the energy required to remove the α hydrogen atom, leaving the geometry of the rest of the molecule unchanged. $\Delta E_{relax,BDE}$ is the energy released when the vertical product relaxes to the optimized radical geometry.

$$\mathrm{BDE} = BDE_{vert} - \Delta E_{relax,BDE} \qquad (12)$$

We observe that BDE_{vert} is maximum for **4H** and minimum for both **6H** and **7H** (Table 4). It is believed that as the size of a carbon containing ring decreases, the smaller ring angles cause increased s-character in the carbon orbitals used to form the external C−H bonds.[1] More s-character leads to a stronger C−H bond, and this is reflected in the increasing BDE_{vert} with decreasing ring size.

The relaxation energy, on the other hand, is smallest in the **4H** system and largest in the **6H** system. This quantity likely tracks the lactone enolate radical's ability to compensate for strain introduced into the ring upon rehybridization of the α-carbon from sp^3 to sp^2. Interestingly, $\Delta E_{relax,BDE}$ for the **7H** system is somewhat less than for **6H**, suggesting that there is more ring strain in **7**• than in **6**•. This is consistent with the additional 6.4 kcal/mol strain in cycloheptane compared with cyclohexane, as with the additional 4.1 kcal/mol strain in cycloheptene compared with cyclohexene.

Adding together the effects seen in both the BDE_{vert} and the $\Delta E_{relax,BDE}$, we can see why the BDE for **6H** is dramatically less than for **4H**. The **4H** system has the largest BDE_{vert} coupled with the smallest $\Delta E_{relax,BDE}$, whereas the **6H** system has the smallest BDE_{vert} coupled with the largest $\Delta E_{relax,BDE}$.

Conclusion

We have measured the gas-phase acidities of lactones with ring sizes between 4 and 7. We have also measured the EAs of the corresponding lactone enolate radicals and derived the αC−H BDEs of the neutral lactones. The relative experimental acidities, EAs, and BDEs are all in good agreement with calculations. The enhanced gas-phase acidity of the lactones over methyl acetate is consistent with the dipole repulsion model used to explain the enhanced solution acidities of lactones over other esters. Hyperconjugation effects from the β-carbon of enolate radicals, in conjunction with the dipole repulsion model, account for the relative EAs of the δ-valerolactone and methyl acetate enolate radicals and also account for the relative BDEs of δ-valerolactone and methyl acetate. A significant dependence on ring size is seen for the EAs and the BDEs but not for the acidities.

Acknowledgment. We are grateful to the National Science Foundation for support of this work. We thank Michael Chabinyc for his assistance with the density functional theory calculations. J.M.K. holds a Franklin Veatch Memorial Fellowship.

JA011897I